An Accurate HEMT Large Signal Model Usable in SPICE Simulators

*Joe Staudinger, **Monte Miller,
**Mike Golio, *Bill Beckwith, ***Dave Halchin

*Motorola Strategic Electronic Division
Chandler, AZ 85248-2899
**Motorola Semiconductor Research and Development Laboratories
Tempe, AZ 85284
*** Motorola Phoenix Corporate Research Laboratories
Tempe, AZ 85283

ABSTRACT

An empirical large signal model which describes HEMT characteristics has been developed, implemented and compared to measured performance. When compared to existing MESFET models, better accuracy is obtained in predicting HEMT transconductance. The validity of the model has been examined by comparing harmonic content predicted by SPICE to measured results.

I INTRODUCTION

In this work a large signal dc HEMT model has been developed and implemented in both a parameter extractor program, GASMAP [1,2]; and a large signal circuit simulator, SPICE. Parameters required by the model have been determined to describe a 0.25 x 60 micron gate pseudomorphic HEMT. The resulting model describes the HEMT performance with significantly greater accuracy than MESFET models which are available on commercial large signal simulators. The validity of the model has been investigated by comparing the measured output power spectrum of the device to that obtained from large signal simulations under identical conditions. The predictive capability of the model is good for some bias conditions, but limited by the deficiencies of the model at high bias currents.

II DEVICE CHARACTERIZATION AND PARAMETER EXTRACTION

Device Characterization:
To aid in the development and validation of the new HEMT model, both S-parameter and DC current-voltage measurements were chosen to characterizing a 0.25 x 60 μm HEMT device. The S-parameters of the device were measured using on wafer probing techniques from 1 to 20 GHz at 40 unique bias conditions. The drain-source and gate-source voltages were chosen to obtain 40 bias states such that the measured S-parameters provided a global representation of the HEMT device characteristics. In addition to S-parameters, DC current-voltage measurements were also measured to further characterize the device.

Parameter Extraction:
To compress the large quantity of characterization data into a more manageable form, the measured S-parameter data at each bias were reduced to small signal equivalent circuits (Figure 1). This was accomplished using a direct extraction method [3]. This information was used, along with DC current voltage characteristics, to determine model parameters.

The parameter extraction technique first described by Miller et al. [4] has been used to obtain large signal model parameters for the HEMT being investigated in this study. This method of parameter extraction simultaneously matches measured and modeled DC drain-source current, rf output conductance, and transconductance. Note that frequency dispersion in both the output conductance and transconductance is considered with this technique. Comparisons illustrating the agreement between measured and modeled HEMT characteristics are discussed in section IV.

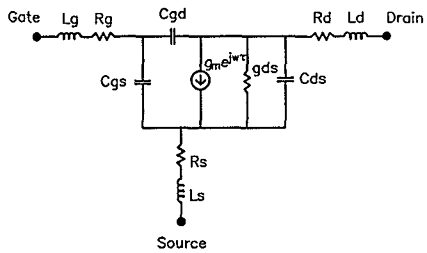

Figure 1 Equivalent small signal circuit model representation of the HEMT.

III HEMT MODEL

Although HEMT devices have already exhibited superior high-frequency and low-noise performance over competing MESFET technology, much less work has been done to produce accurate large signal HEMT models which are compatible with large signal circuit simulator routines. In choosing an accurate HEMT model for implementation into a large signal simulator, the model must predict large signal performance by predicting voltage dependance of device characteristics.

The HEMT model chosen for implementation is based on a MESFET model developed by Meta-Soft [6] with certain modifications required for HEMTs [1,2]. One of the most significant differences between MESFETs and HEMTS is in the device transconductance. Additionally, transconductance is a device parameter which is often most critical in predicting other large signal effects.

The device expressions for the HEMT consider two regions of gate-source voltage.

for $V_{gs}<V_{pf}$:

$$I_{ds} = \beta_{eff}(V_{gst}{}^{VGEXP})(1 + \lambda V_{ds})\tanh(\alpha V_{ds}) \quad (1)$$

$$g_m = I_{ds}((VGEXP/V_{gst}) - \mu_{crit}/(1 + \mu_{crit} V_{gst})) \quad (2)$$

$$g_{ds} = \beta_{eff}(V_{gst}{}^{VGEXP})(1 + \lambda V_{ds})(\alpha/\cosh^2(\alpha V_{ds})) + \beta_{eff}(V_{gst}{}^{VGEXP})\lambda\tanh(\alpha V_{ds}) - g_m\gamma \quad (3)$$

and for $V_{gs}>V_{pf}$:

$$I_{ds} = \beta V_{gst}{}^{VGEXP}(1+\lambda V_{ds})\tanh(\alpha V_{ds}) - \beta_{eff}\xi(V_{gs}-V_{pf})^{\Psi}(1+\lambda V_{ds})\tanh(\alpha V_{ds}) \quad (4)$$

$$g_m = \beta_{eff}V_{gst}{}^{VGEXP}(1+\lambda V_{ds})\tanh(\alpha V_{ds})(VGEXP/V_{gst} - \mu_{crit}/(1+\mu_{crit}V_{gst})) - \beta_{eff}\psi(V_{gs}-V_{pf})^{\Psi}(1+\lambda V_{ds})\tanh(\alpha V_{ds})(\psi/(V_{gs}-V_{pf})) - (\mu_{crit}/(1+\mu_{crit}V_{gst})) \quad (5)$$

$$g_{ds} = \beta_{eff}(V_{gst}{}^{VGEXP})(1 + \lambda V_{ds})(\alpha/\cosh^2(\alpha V_{ds})) + \beta_{eff}(V_{gst}{}^{VGEXP})\lambda\tanh(\alpha V_{ds}) - g_m\gamma - \beta_{eff}\xi(V_{gs}-V_{pf})^{\Psi}(1+\lambda V_{ds})\tanh(\alpha V_{ds})((\mu_{crit}\gamma)/(1+\mu_{crit}V_{gst})) + (\lambda/(1+\lambda V_{ds})) + (\alpha(1-\tanh^2(\alpha V_{ds}))/\tanh(\alpha V_{ds}) \quad (6)$$

In addition to the current-voltage relationship, the capacitance-voltage characteristics for HEMTs must also be considered. For the initial evaluation, the current Statz [5] model, which is commonly used for MESFETs, was chosen. This choice proved adequate even though the fit to the HEMT is generally poorer than to MESFET devices.

IV MEASURED AND MODELED HEMT CHARACTERISTICS

Figure 2 shows the agreement between measured and modeled dc current-voltage relationships. The agreement is seen to be good for currents below about 10 mA but to differ significantly for higher bias conditions. Some sacrifice is made in the agreement between these dc characteristics in order to improve the agreement in the measured and modeled rf device characteristics. This compromise is necessary because of the existence of dispersion in the behavior of HEMTs at low frequencies.

Figure 3 illustrates the predicted output conductance of the model with the measured rf output conductance of the device. The agreement is seen to be better at higher current drive levels than at very low levels (ie. less than 1 mA). The modeled output conductance for V_{gs} = 0.1 V, for example, does not predict the observed drop in conductance for low V_{ds} values.

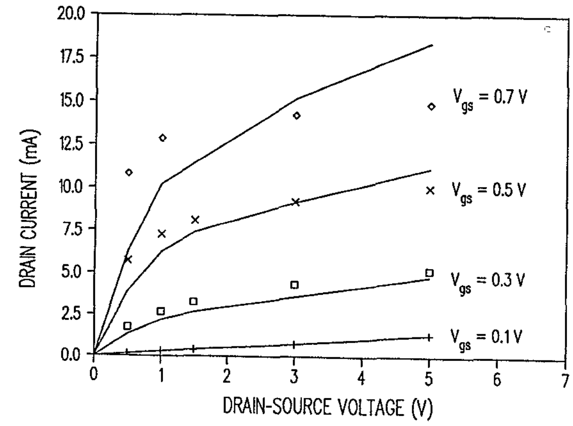

Figure 2 Measured and modeled DC current-voltage relationships for a 0.25 x 60 micron gate pseudomorphic HEMT.

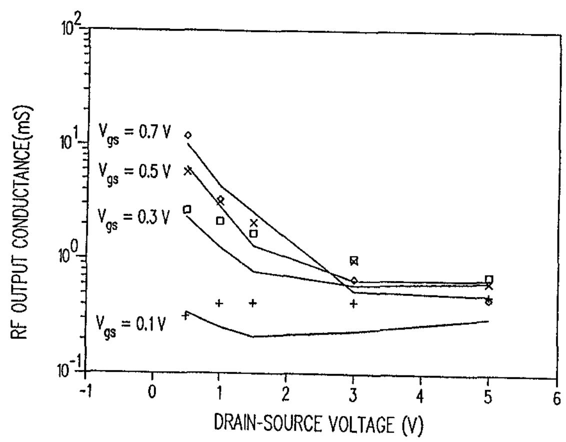

Figure 3 The output conductance predicted by the HEMT model is compared to extracted values of conductance for a 0.25 x 60 0.25 x 60 micron gate pseudomorphic HEMT.

Figure 4 presents a comparison between the modeled transconductance and the intrinsic transconductance measured at microwave frequencies. The model is seen to accurately predict performance for low values of gate-source voltage and also to exhibit transconductance degradation for higher V_{gs} values. Significant differences are seen, however, between the observed and modeled g_m degradation properties. The HEMT model developed and employed in this work degrades the computed transconductance for gate-source voltage levels above a fixed voltage, V_{pf}. In the current model, this voltage is independent of drain-source voltage. In the characteristics observed for this particular device, however, the onset of transconductance dispersion occurs at lower gate-source voltage levels when higher drain-source voltages are utilized. The discrepancy between measured and modeled characteristics was found to be more severe for other drain-source bias levels not shown. Despite this deficiency in the present model, the agreement observed is significantly superior to that obtained using MESFET models. It should also be noted that the gate-source voltage dependance of the onset of transconductance degradation observed in this device has not been found to be common to all HEMT devices.

Figure 5 presents the observed agreement between measured and modeled device capacitance. The model proposed by Statz et al. [5] for MESFETs has been applied to this problem. The agreement between measured and modeled gate-drain capacitance is seen to be very good. The gate-source capacitance characteristics are not modeled as accurately as the gate-drain capacitance with this model.

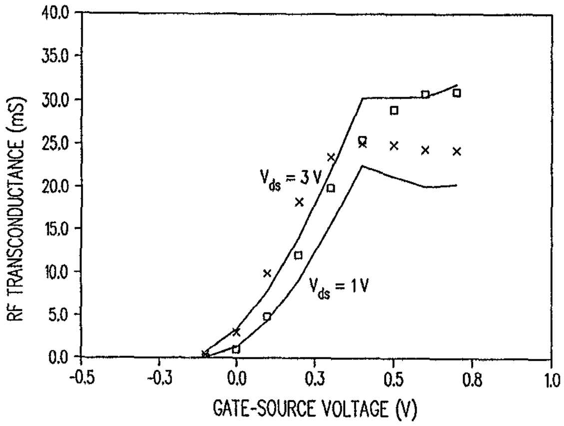

Figure 4 A comparison between the modeled transconductance and the intrinsic transconductance measured at microwave frequencies.

V MEASURED AND MODELED LARGE SIGNAL PERFORMANCE

The new HEMT model was added to the circuit simulator PSPICE by including Eqs. (1)-(6) and utilizing the existing Statz model for the device capacitance. The validity of the model was examined by comparing the spectral content of an amplified signal as predicted by SPICE to actual measurements. These measurements were made with the HEMT embedded in a 50 ohm system. A signal was applied to the gate of the HEMT and the resulting spectral content of the drain-source voltage (V_{ds}) was measured with a spectrum analyzer.

The agreement between the measured and simulated output power spectrum of the device when biased at I_{ds} = 5 mA is illustrated in Figure 6. The model is seen to predict fundamental and third harmonic content with good accuracy, but to be less accurate for second and fourth harmonic levels. At this current, the required gate-source bias voltage is very close to V_{pf}.

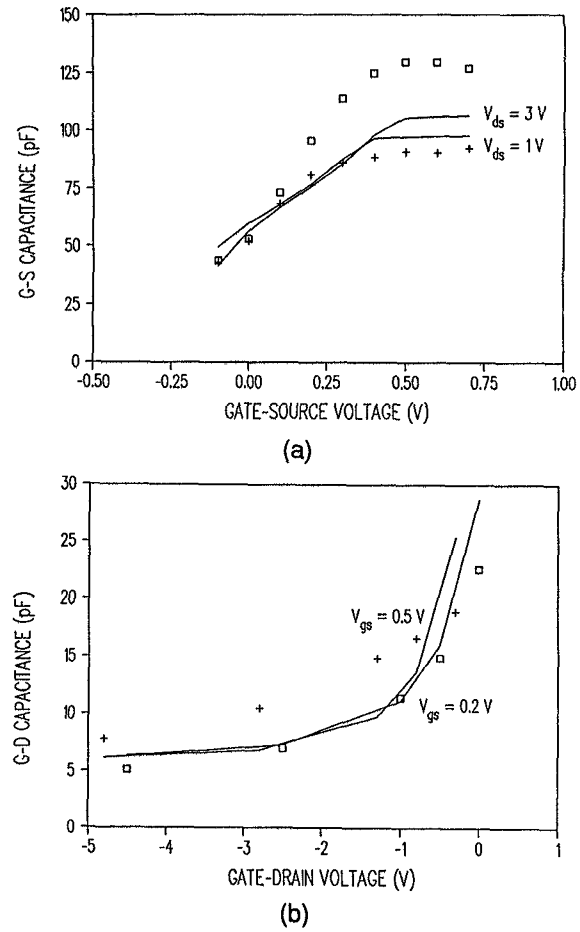

Figure 5 Observed agreement between measured and modeled device capacitance. The model proposed by Statz et al. [5] for MESFETs has been applied to this problem. a) Gate-source capacitance. b) Gate-drain capacitance.

The measured and simulated output power spectra are compared for a bias level of I_{ds} = 10 mA (well beyond the onset of transconductance degradation) in Figure 7. Although the prediction of fundamental and third harmonic levels are marginally acceptable for a wide range of input power levels, the predicted second harmonic level is seen to be poor. This deficiency is probably due to the inability of the model to accurately predict the transconductance degradation behavior at the higher bias levels.

CONCLUSION

A large signal HEMT model has been developed and implemented within a parameter extractor program and SPICE. The model predicts HEMT behavior significantly better than existing MESFET models, but also exhibits some deficiencies at high bias levels. The parameter extraction results indicate that the addition of a V_{ds} dependant critical voltage for the onset of transconductance degradation may improve the model.

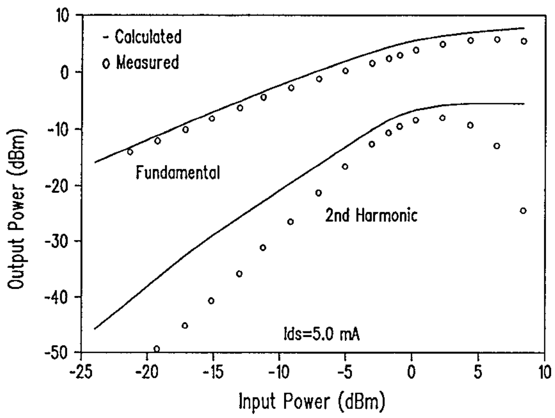

(a)

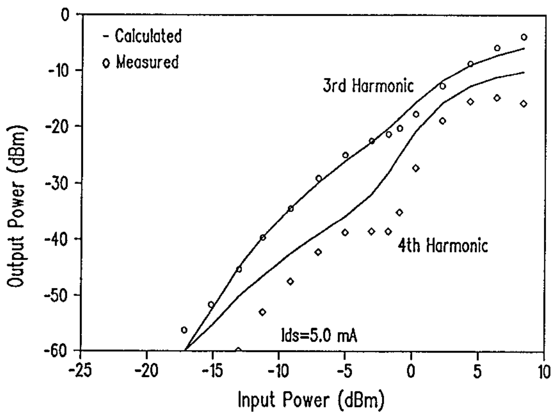

(b)

Figure 6 Measured and simulated output power spectrum of the device when biased at I_{ds} = 5 mA and V_{ds} = 4.0 Volts. a) Fundamental and 2nd harmonic. b) 3rd and 4th harmonics.

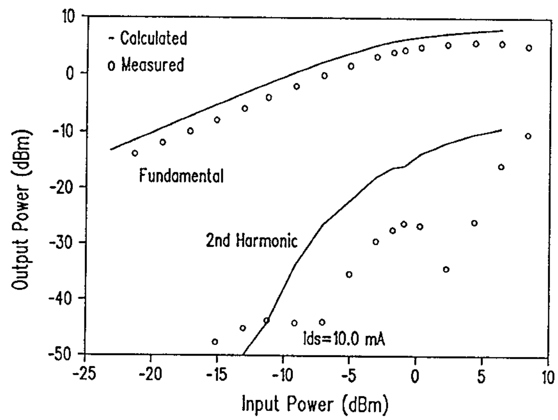

(a)

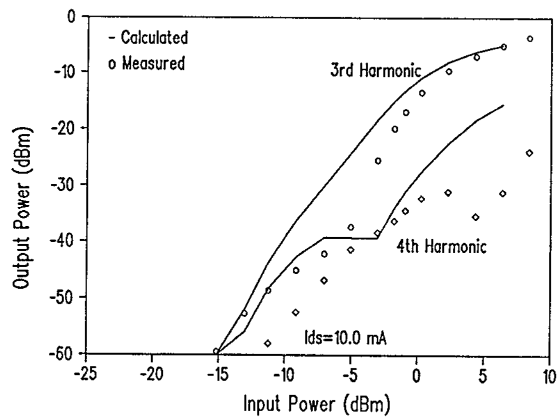

(b)

Figure 7 Measured and simulated output power spectrum of the device when biased at I_{ds} = 10 mA and V_{ds} = 4.0 Volts. a) Fundamental and 2nd harmonic. b) 3rd and 4th harmonics.

A comparison between measured large signal performance and predictions obtained from simulations shows that the model can be used to obtain large signal behavior of HEMT devices for some bias conditions, but may be limited when high bias levels are used.

References

[1] Microwave MESFETs and HEMTs: Characterization, Parameter Extraction and Modeling for CAD Applications, ed. J. M. Golio, Artech House, February 1991.

[2] J. M. Golio, M. Miller, E. Arnold, B. Beckwith, GASMAP: Gallium Arsenide Model Analysis Program, User's Manual, distributed by Artech House, March 1991.

[3] E. Arnold, J. M. Golio, M. Miller, B. Beckwith, "Direct Extraction of GaAs MESFET Intrinsic Element and Parasitic Inductance Values," IEEE MTT-S International Microwave Symposium Digest, pp. 359-362, May 1990.

[4] M. Miller, J. M. Golio, B. Beckwith, E. Arnold, S. Ageno, S. Dorn, "Choosing an Optimum Large Signal Model for GaAs MESFETs and HEMTs," IEEE MTT-S International Microwave Symposium Digest, pp. 1279-1282, May 1990.

[5] H. Statz, P. Newman, I. Smith, R. Pucel, H. Haus, "GaAs FET Device and Circuit Simulation in SPICE,", IEEE Trans. on Elec. Devices, vol. ED-34, pp. 160-169, 1987

[6] HSPICE User's Manual, (Version H8907), Meta-Software, Campbell, CA 95008, 1989